$$\frac{U_*''}{U} = A_1 + B_1 \log \frac{\Psi'}{\alpha} \tag{7.59}$$

for which, the coefficients A_1 and B_1 and the parameter α are listed in Table 7.2.

Table 7.2 shows that for $\omega D/\upsilon > 100$ (for normal water temperature, this value corresponds to a natural sediment size greater than 1 mm), ripples do not form on a bed, and the bed configuration is mainly that of dunes. In this case, the flow parameter ψ' plays a determinant role. For $\omega D/\upsilon < 100$, because Shen's analysis is based mainly on a large amount of flume experiment data, the bed configuration is mostly in the form of ripples. In this case, in addition to the parameter ψ', the Reynolds number $\omega D/\upsilon$ must be included. Chapter 6 shows that the two key parameters are the flow parameter ψ' and the grain Reynolds number $U_* D/\upsilon$. If the bed configuration is in the ripple-dune phase, the effects of the flow parameter ψ' and the grain Reynolds number should both be used in determining the bed form resistance.

Table 7.2 Values of coefficients and parameter used in Eq. (7.59) (after Shen, H.W.)

$\omega D / \upsilon$	ψ'	A_1	B_1	α
>100	<10	0.03	+0.01	7.12
	>10	0.06	-0.09	7.12
1—100	—	0.03	+0.11	$=(\omega D / \upsilon)^{1/2}$

3. Engelund method [33]. Engelund used the flow parameters suggested by Einstein. His method is considered to be reliable, particularly in Europe, and is widely used there. Hence, its derivation should be presented and compared with Einstein method.

First, following Mayer-Peter's work, Engelund divided the bed resistance τ_b in 2-D alluvial streams into grain friction τ_b' and bed form resistance τ_b'' according to the energy slope,

$$\tau_b = \gamma h J = \tau_b' + \tau_b'' = \gamma h J' + \gamma h J'' \tag{7.60}$$

For grain friction, Engelund suggested

$$\tau_b' = \gamma h J' = \gamma h' J$$

For bed form resistance, the resistance loss can be written much as in Eq. (7.52). If each resistance component is replaced by the corresponding Darcy-Weisbach coefficient of resistance, then Eq. (7.60) can be written as

$$f_b = f_b' + \frac{4\alpha\Delta^2}{h\lambda} \tag{7.61}$$

Furthermore, Engelund introduced a parameter for the flow intensity

$$\Theta = \frac{hJ}{\frac{\gamma_s - \gamma}{\gamma} D} \tag{7.62}$$

This parameter is simply the inverse of the Einstein flow parameter, ψ'. Correspondingly,

$$\Theta' = \frac{h'J}{\frac{\gamma_s - \gamma}{\gamma} D} \tag{7.63}$$

and,

$$\Theta'' = \frac{1}{2} F_r^2 \frac{\alpha\Delta^2}{\frac{\gamma_s - \gamma}{\gamma} D\lambda} \tag{7.64}$$

in which,

$$Fr = \frac{U}{\sqrt{gh}}$$

Now Eq. (7.60) can be written as

$$\Theta = \Theta' + \Theta''$$

Engelund next presented his similarity hypothesis; namely, if two rivers (denoted by subscript 1 and 2) are dynamically similar, they must meet the following two criteria:

First, the effective shear stresses on these beds must be equal ($\Theta_1' = \Theta_2'$);

Second, the ratios of local enlargement losses caused by bed configuration to total energy loss must be equal.

From the second criterion,

$$f_{b1} / f_{b2} = f'_{b1} / f'_{b2} \tag{7.65}$$

Since

$$f'_b / f_b = \Theta' / \Theta$$

So

$$\Theta_1 / \Theta_2 = \Theta'_1 / \Theta'_2 \tag{7.66}$$

From the first criterion

$$\Theta'_1 = \Theta'_2, \Theta_1 = \Theta_2$$

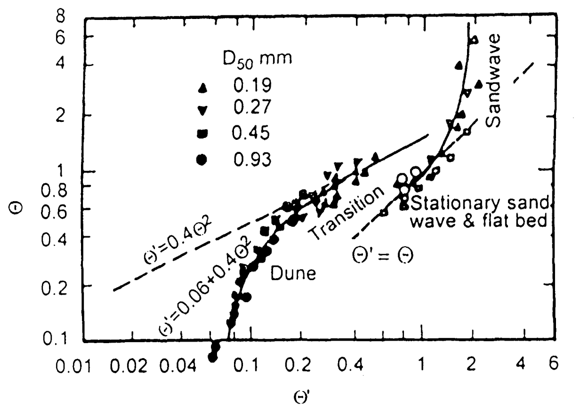

Fig. 7.33 Relationship between grain friction and total bed resistance (after Engelund, F., and E. Hansen.)

Hence, if Θ is a function of only Θ', Eq. (7.66) is tenable,

$$\Theta = f(\Theta') \tag{7.67}$$

From the foregoing analysis, Engelund plotted the $\Theta \sim \Theta'$ curve using data from flume experiments, as shown in Fig.7.33. In the dune phase,

$$\Theta' = 0.06 + 0.4\Theta^2 \tag{7.68}$$

As Θ decreases, Θ' gradually approaches the constant value of 0.06, which corresponds to the condition of incipient motion. If $\Theta > 0.4$,

$$\Theta' = 0.4\Theta^2 \tag{7.69}$$

In contrast, for high transport rates of sediment and with sand waves forming on the bed, the data fall near the other curve. For flat bed or for stationary sandwaves without local enlargement loss,

$$\Theta' = \Theta$$

But in the sand wave phase, as a result of the additional energy loss caused by the breakage of the water surface, Θ' is smaller than Θ. Engelund was able to express the resistance losses for all

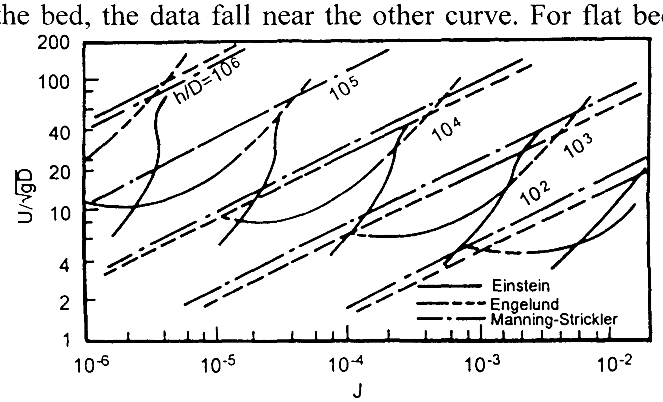

Fig. 7.34 Comparison of resistance formulas (after Chollet, J.P., and J.A. Cunge)

phases of bed configuration, except for the ripple phase, in a single figure.

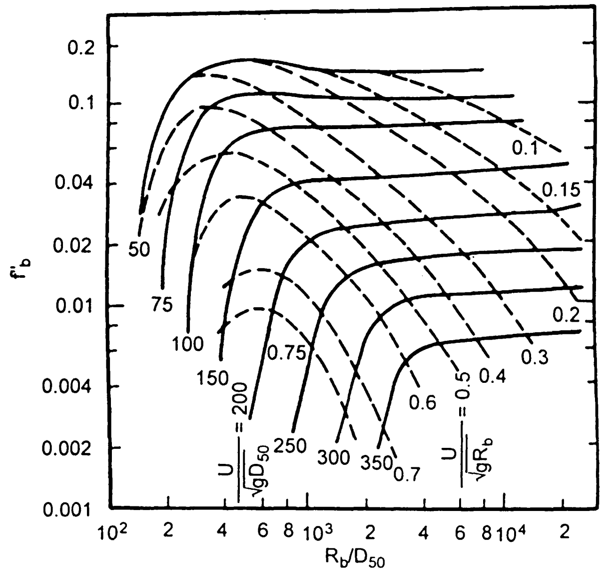

Fig. 7.35 Relationship between bed form resistance, Froude number and relative roughness (after Alam, A.M.Z., and J.F. Kennedy)

Because Engelund and Einstein used the same flow parameter to express the bed form resistance, the two methods can be readily compared. After some mathematical transformation, Chollet and Cunge expressed the equations of Einstein, Engelund, and Manning-Strickler as relationships between $U/\sqrt{gD}$ and J with h/D as a third parameter, as shown in Fig.7.34 [48]. The figure shows that

(1) The Manning-Strickler formula expresses only grain friction, and should not be used for flows with bed forms;

(2) If the bed is flat, the trend of the three formulas is essentially the same: a straight line with a slope of 1/2. The different formulas used to express the mean velocity did not affect the results significantly;

(3) Because Engelund included results both high and low sediment transport rates, the formation of a flat bed was possible; hence, the two ends of his curve fall on the straight line with a slope of 1/2. But the Einstein formula includes only dune resistance; if the sediment transport rate is high and dunes tend to disappear, the curve intersects with the straight line with a slope of 1/2. For a low sediment transport rate, the curve does not automatically transfer into the resistance formula for a flat bed;

(4) In the dune phase, if the bed is fairly steep and the relative roughness (*D/h*) is large, the Einstein and Engelund formulas differ very little; but for streams in an alluvial plain with small relative roughness, the difference between them is quite large.

4. Alam and Kennedy method [49]. Among the formulas for bed form resistance, some include the Froude number and relative roughness as parameters. The work of Alam and Kennedy is representative of this type.

They used the curves in Fig. 7.29 to obtain the grain friction, and then the principle of summation of component resistances to obtain the corresponding bed form resistance. They plotted the curve for the bed form resistance coefficient against $U/\sqrt{gR_b}$, using R_b/D_{50} as a third parameter, as shown in Fig. 7.35. In the same figure, they plotted curves for $U/\sqrt{gD_{50}}$ as a third parameter. For large rivers, the plots of $U/\sqrt{gD_{50}}$ are straight lines parallel to the abscissa, which indicates that bed form resistance is not related to the relative roughness but depends mainly on a Froude number of the type of $U/\sqrt{gD_{50}}$. In small rivers and flumes, both $U/\sqrt{gD_{50}}$ and R_b/D_{50} affect the bed form resistance significantly.

7.5.3 Bank resistance

The bank resistance can usually be estimated using the Manning equation:

$$U = \frac{1}{n_w} R_w^{2/3} J^{1/2}$$

in which the bank roughness n_w depends on the material in the bank wall and can be obtained from roughness tables like Table 7.3:

Table 7.3 Bank roughness coefficient

Situation of banks	n_w	
	range	common value
Cement pavement	0.011—0.015	0.013
Stone blocks paved with cement	0.017—0.030	0.025
Dry rock paving	0.025—0.035	0.030
Smooth ground banks	0.017—0.025	0.0225
Ground banks with weed	0.027—0.035	0.030
Sand and gravel banks	0.020—0.030	0.027
Gravel banks	0.025—0.030	0.030

In irrigation canals, artificial methods are sometimes used to promote the deposition of fine sediment in a certain stretch to prevent the banks from scouring. In such cases, the material of the banks is mostly fine sediment, and the bank surface is smooth enough that it can be treated as hydraulically smooth as already discussed. However, in mountain rivers, especially in gorges reaches with high and precipitous banks and a low ratio of width to depth, the bank roughness is often quite large. For instance, in the river reaches of Wuxia Gorge and Qutangxia Gorge of the Yangtze River, the Manning roughness coefficient for the bank can exceed 0.10.

7.5.4 Floodplain resistance

The vegetation on floodplains includes grasses, brush, trees, and even forest. When the flood reaches the floodplains, the resistance to flow is mainly either ordinary friction or form resistance due to vegetation. In some of the older textbooks on hydraulics, the vegetation density was used to determine the roughness. Now, however, the use of only this one parameter to indicate the effect of vegetation on resistance is known to be far from sufficient. More studies of this aspects have been made, but the results do not provide a final solution.

The study of the effect of vegetation on resistance needs to reflect two quite different situations. Depending on the flow velocities and the stiffness of the vegetation, grasses and brush can either stand up or bend over. In the first situation, the roughness is comparable to that of large-sized particles protruding out from bed, and the resistance is related to the projected area and the vegetation density. For the second, the bed can have an undulating shape that may fall within the hydraulically smooth region for turbulent flow. In this latter case, the resistance can be affected somewhat by the Reynolds number. But, if the flow depth is less than the vegetation height, the result is more like the first case.

7.5.4.1 Prone vegetation

The first scientists to study systematically the flow capacity of canals with vegetation were Ree and Palmer [50]. They found that as the flow velocity increases, vegetation progressively bends over and the resistance continuously decreases. Using the concept of relative roughness, they established a correlation between the canal roughness and the product of mean velocity U and hydraulic radius R, as shown in Fig.7.36. Various types of vegetation with different heights fall on different curves. Later, Kouwen and Unny conducted flume experiments using styrene strips 10 cm long, 0.5 cm wide, and 0.3 mm thick to simulate vegetation, and they identified the two primary strip positions as vertical and horizontal [51]. If the styrene strips were fully bent over, the bed was more or less hydraulically smooth and the resistance coefficient varied with the Reynolds number. Their data, in Fig. 7.36, coincided closely with the results of Ree and Palmer. As the viscosity of water varies little for normal conditions, the parameter UR can be used in place of the Reynolds number for the abscissa in the figure. That is, if the vegetation is quite pliable, it bends over with the flow, and the bed becomes either hydraulically smooth or within the transition region from hydraulically smooth to rough. Morris called this region quasi-smooth and suggested that it is like a continuous bed with individual, scattered resistance components [52].

If water flows over floodplains covered by vegetation, the velocity is often rather low so that the flow can be laminar. For this case, the relationship between resistance coefficient and Reynolds number is that shown in Fig. 7.37[53]. Although the resistance coefficient is then inversely proportional to the Reynolds number, the constant of proportionality is much larger than that for a relatively stable bed formed of glued sand particles, and it increases with the ground slope J_0,

$$f = \frac{510000 J_0^{0.662}}{R_e} \qquad (7.70)$$

The coefficient of proportionality in the relationship between the resistance coefficient and the Reynolds number is not equal to 24 for low flow. This change with bed roughness has been reported in several studies of flow over a bed covered by vegetation, but the reason for the coefficient to be so large and to vary with ground slope is still unknown. The data of Ree and Palmer, Kouwen and Unny are also shown in Fig.7.37. The trend of the data indicates that their experimental results fall within the transitional region between laminar and turbulent flow. For the same Reynolds number and ground slope, the resistance of a trapezoidal cross-section appears to be larger than that for a rectangular cross-section.

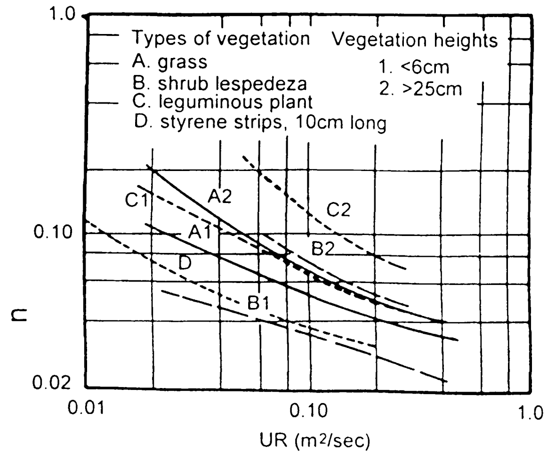

Fig. 7.36 Relationship between the roughness, vegetation and flow condition in channels with vegetation (after Ree,W.O., and V.J. Palmer)

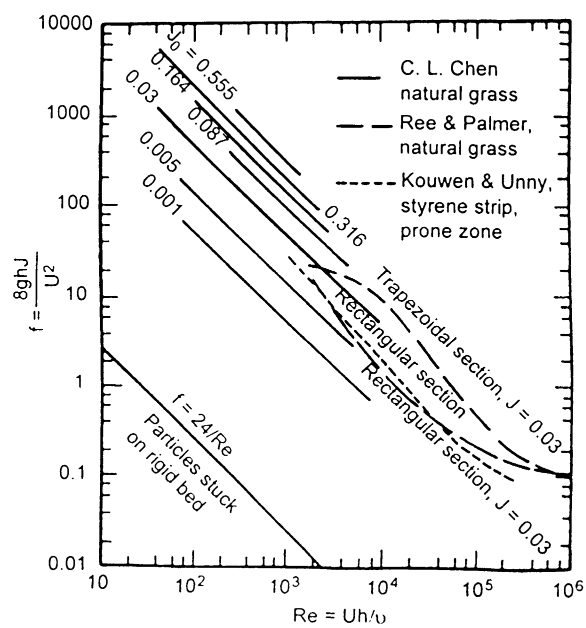

Fig. 7.37 Relationship between resistance coefficient and Reynolds number on a bed covered with vegetation (in laminar and transitional regions) (after Chen, C.L.)

7.5.4.2 Standing vegetation

For vegetation standing up straight, the vertical velocity distribution is that shown in Fig. 7.38a. The vegetation height is k, and the velocity at that level is u_k. For the experimental data with styrene strips, u_k is a function of the friction velocity U_*, the data for the vegetation are concentrated on separate belts. In the main flow above the vegetation, the velocity distribution follows the usual logarithmic law, and forms a straight line on semi-logarithmic paper (Fig. 7.38c).

Kouwen and Unny found that the flow over standing vegetation was similar to that over a rough surface. The resistance loss does not vary with the Reynolds number and thus depends only on the relative roughness k/h. The measured data are shown in Fig. 7.39. The range of the Reynolds numbers in the experiment was not large enough to define the curve fully, especially if the vegetation extends nearly to the surface. In fact, the phenomenon is more complex than that shown in Fig. 7.39. The resistance loss caused by standing vegetation, somewhat like that for large protruding roughness on a bed, is mainly dependent on the projected area of vegetation normal to flow and the vegetation density. For scattered vegetation, each tree or blade of grass has its individual resistance. With a greater density of vegetation, the wakes caused by separation on the lee side tend to overlap. Once the vegetation covers the plane surface, the flow contacts only the tops of the vegetation; it is therefore still hydraulically rough, but the roughness size is certainly less than the bended height k. Petryk and Bosmajian III studied the resistance for flow depths smaller than the vegetation height [54], and derived the expression

$$n = n_b \sqrt{1 + \frac{C_D}{2g} e' (\frac{1}{n_b})^2 R^{4/3}} \tag{7.71}$$

in which, n_b is bed surface roughness excluding the effect of vegetation, C_D the resistance coefficient due to vegetation, e' the vegetation density

$$e' = NA' / A \tag{7.72}$$

N is number of trees on bed area A, A' the projected area of trees normal to the flow.

If the resistance is mainly induced by vegetation, Eq. (7.72) can be simplified to

$$n = R^{2/3} \sqrt{\frac{C_D}{2g} e'} \tag{7.73}$$

Eqs. (7.71) and (7.72) should be used only for scattered vegetation without mutual disturbance.

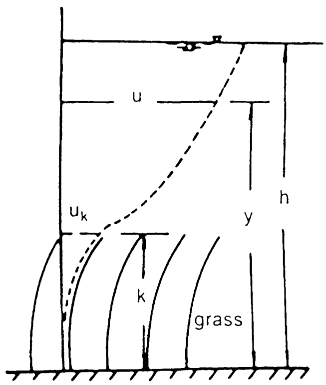

(a) Sketch of velocity distribution

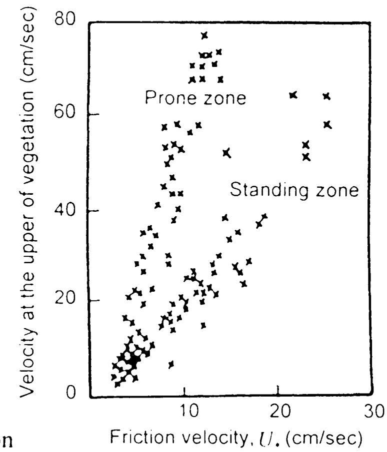

(b) Result of simulation experiments

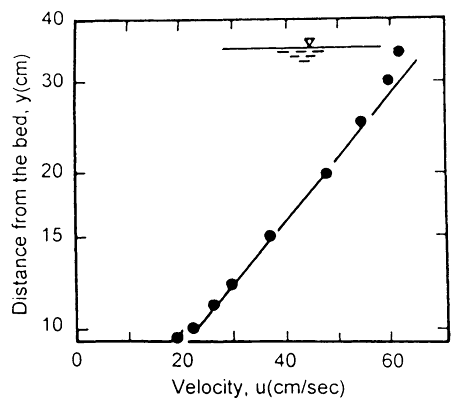

(c) Measured velocity distribution in main flow region

Fig.7.38 Vertical velocity distribution for a bed covered by vegetation (after Kouwen, M., and Y.E. Unny)

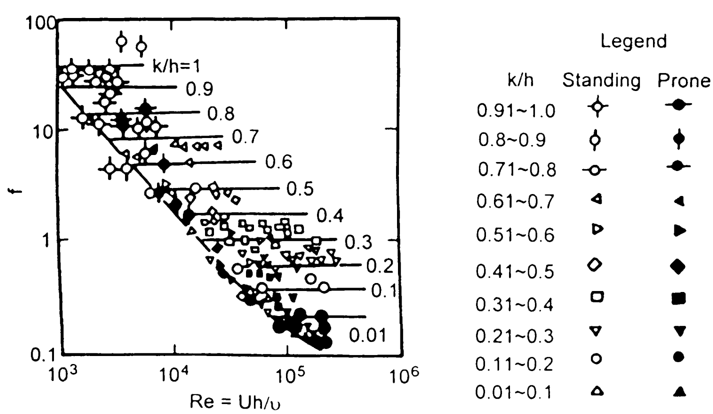

Fig. 7.39 Resistance due to vegetation (after Kouwen, M., and Y.E. Unny)

The above analysis shows that the variation of roughness with flow depth is closely related to the distribution of projected area of vegetation on a vertical plane. If the vegetation resistance is mainly due to tree stems, and the stem diameter does not vary significantly over the depth, or if the decrease in stem diameter with increasing depth tends to be affected by the increase in branches and leaves, the roughness coefficient is proportional to the 2/3 power of R. In contrast, if the area of the vegetation decreases with the increasing flow depth, so that it is inversely proportional to the 3/4 power of R, then the roughness coefficient may not change much with water level and is approximately constant. The field data show that both of these situations occur as well as a transition between them, from the type of vegetation and the season, one can determine the vegetation density and the resistance it presents.

7.6 COMPREHENSIVE RESISTANCE FORMULAE

The method for determining a composite resistance from resistance elements presented in the foregoing section is quite complex. Sometimes, however, one does not need to know grain friction and its corresponding hydraulic radius, but wants to know the discharge that passes through a cross-section with a certain slope. A relatively simple and comprehensive resistance formula can be used for the latter purpose.

7.6.1 Chien-Mai comprehensive resistance formula [38]

Chien and Mai used the Manning-Strickler formula in the form

$$U = \frac{A}{K_s^{1/6}} R^{2/3} J^{1/2}$$

If $K_S = D_{65}$, and if the cross-section is wide and shallow so that the bank resistance is negligible, the formula can be written in the form

$$U = \frac{A}{D_{65}^{1/6}} h^{2/3} J^{1/2} \tag{7.74}$$

They did not treat A as constant but related it to the factors that dominate the evolution of sand waves. As a first approximation, they expressed A as a function of the flow parameter ψ' [Eq. (7.58)]; Fig. 7.40 presents the results of the data for the Lower Yellow River in this form. If the velocity is low, the sediment transport rate not high, and the corresponding ψ' value quite large, the parameter A is small because of the action of bed form resistance or other channel form resistance. If ψ'